A R C H I V E S O F M E T A L L U R G Y A N D M A T E R I A L S
Volume 50 2005 Issue 4

F. STACHOWICZ*, P. LITWIN*, W. FRĄCZ*

# EXPERIMENTAL AND NUMERICAL STUDY OF OPEN STRUCTURAL PROFILE BENDING PROCESS

# EKSPERYMENTALNA I NUMERYCZNA ANALIZA PROCESU GIĘCIA OTWARTYCH PROFILI KONSTRUKCYJNYCH

Determination of the bending moment and springback coefficient of thin- walled open structural profiles, as a function of the bending curvature was the main objective of the work. The experiment was carried out using angle- section beams (L-shape) made of St3S common steel and channel-section beams (U-shape) made of PA38 aluminium alloy. Distortion of cross section, which affects bending process of thin wall products, was analyzed and discussed. The MARC computer code was used for the bending process simulation. Experimental and simulated bending characteristics, bending moment as a function of bending curvature as well as springback coefficient as a function of bending radius, were compared.

Celem podjętych badań było określenie momentu gnącego oraz współczynnika sprężynowania w funkcji krzywizny gięcia otwartych profili cienkościennych. Badania doświadczalne przeprowadzono dla kątowników (profil typu L) wykonanych ze stali St3S oraz ceowników (profil typu U) wyciskanych ze stopu aluminium PA38. Przeanalizowano wpływ zniekształcenia przekroju poprzecznego na proces gięcia profili cienkościennych. Do symulacji procesu gięcia zastosowano komercyjny program komputerowy MSC MARC. Dokonano porównania charakterystyk gięcia, momentu gięcia w funkcji krzywizny gięcia oraz współczynnika sprężynowania w funkcji promienia gięcia, wyznaczonych eksperymentalnie oraz na drodze obliczeń numerycznych.

## 1. Introduction

The application of beams of open cross-section have recently become increasingly demanding. From a structural engineer's point of view, building and construction (wall panels, window, scaffolding, offshore structures) and transportation (automotive, trains,

* POLITECHNIKA RZESZOWSKA, 35-959 RZESZÓW, AL. POWSTAŃCÓW WARSZAWY 8

sea vessels, aerospace) are the most interesting fields. Although it may seem quite straightforward to bend a thin-walled open profile to a desired curvature, several difficulties may arise in industrial bending operations. The most important is cross-section deformation — sagging of beam wall causes limitation of minimum bending radius. In the case of the circular cross- section tube bending, the parameter describing the degree of cross-sectional deformation is the degree of ovalization, and many reports describing this phenomenon could be find in literature, e.g. [1]. When the open structural beams are concerned, it is not possible to determine a similar unique parameter because of the complex shape of the cross-section after bending (Fig.1). Very few studies have been conducted on the plastic bending of open section structural profile — L-shape angle-section beams [2, 3], U-shape channel-section beams [4] and T-shape tee-section beams [5], and the effect of cross-sectional deformation on the main bending parameters is still an open problem. Cross-sectional deformation in conjunction with the strain hardening of a beam material affected the moment-curvature characteristic.

Springback phenomenon is the next important cold bending parameter. The evaluation of elastic springback effect is a fundamental aspect in the practice of bending operations. Springback, in fact, introduces deviations from the desired final shape — consequently, the stamped profile does not conform to the design specifications and could result unsuitable for the application. Since almost all the sheet forming processes are characterized by a significant amount of deformation introduced by a bending mechanics, the distribution of strain along the beam section is strongly inhomogeneous. Such a distribution, together with the elastic-plastic behavior of the workpiece determines the occurrence of springback after removal of the forming tools [5, 6]. It is well known from the tensile test that the elastic part of the total strain, which is recovered if the load is released, is equal to the ratio of the stress before unloading to the Young modulus. The tendency to elastic springback increases at increasing the strain hardening coefficient and at decreasing the elastic stiffness [7]. A complete knowledge of the springback phenomenon and its dependence on material and process variables is strongly required in order to develop effective real time process control systems.

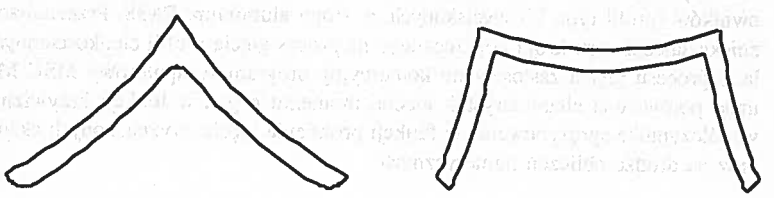

Fig. 1. Cross-section deformation of L-shape and U-shape beams as a result of bending

Controlling the process with respect to repeatability and bendability represents a great challenge in developing competitive design concepts. Traditionally, experimental trial-end- error is required to design, select the process variables, and profile geometry and tooling. Unfortunately, in today's industrial practice, past experience and trial-end-error methods which are being used for finding a suitable procedure

for fabricating structural beam become inefficient and wasteful especially when high productivity is one of the major object. Therefore, there is a great need to replace the experience based techniques by cost-effective knowledge based on compute-aided technique to improve productivity. The development of numerical tools such as the Fine Element Method offers new possibilities for attaining further and more generally applicable knowledge on the bending process. However, numerical simulation of forming processes is a rather delicate task involving large deformations, material non-linearities and contact challenges [8]. Therefore, laboratory test data must be used to validate the numerical model.

In this paper main bending parameters, the bending moment, cross-section distortion and springback coefficient has been examined experimentally under four roll bending test for several L-shaped and U-shaped open section structural beams. The computer code MSC MARC was used to simulate the bending process under pure external moment condition. Experimental results were used for comparison with the finite element simulations, to verify the efficiency of strain hardening models and numerical technique applied in calculations.

## 2. Materials and experimental procedure

Several types of open section structural beams were used in present investigation as test materials (Table 1):

— six types of L-shape angle-section beams — the PA38 aluminium alloy extrusions,

— eight types of U-shape channel-section beams made of St3S common steel — for produced in hot rolling process (Lh- symbol) and four produced in cold sheet bending process (Lc- symbol).

When the mechanical testing is concerned, tensile specimens of 240 mm gauge length and 12.5 mm width were prepared from profile walls. On the base of tensile testing the strain- stress relation in the case of PA38 aluminium alloy was successfully described using Hollomon equation in the form of: $\sigma = C\varepsilon^n$. The values of same mechanical properties were found as follow:

— yield stress — $R_e$ = 89 MPa,

— ultimate strength — $R_m$ = 165 MPa,

— Young's modulus — E = 80.7 GPa,

— strain hardening coefficient — C = 292 MPa,

— strain hardening exponent — n = 0,212.

In the case of the St3S common steel tensile testing a wide quasi-constant plastic range was observed (Fig. 2), and because of that, a kind of multi-function was used to describe strain stress relation:

1. For the elastic range: $\sigma = E\varepsilon$;
2. For the quasi-constant plastic range: $\sigma = R_e(1 + \varepsilon)$;
3. For work hardening range the Krupkowski-Swift equation — $\sigma = C(\varepsilon_0 + \varepsilon)^n$.

TABLE 1

Shape and dimension of constructional profile used in experiment

| Symbol | | Height H mm | Width B mm | Wa ll thickness t mm |
|---|---|---|---|---|
| Channel-section beams (U-shape) made of aluminium alloy | | | | |
| U-15×15×2 | | 15 | 15 | 2 |
| U-30×15×2 | | 15 | 30 | 2 |
| U-30×20×2 | | 20 | 30 | 2 |
| U-40×20×2 | | 20 | 40 | 2 |
| U-25×27×2,5 | | 27 | 25 | 2,5 |
| U-25×27×3 | | 27 | 25 | 3 |
| Angle-section beams (L-shape) made of common steel | | | | |
| Hot rolled | Lh-20×20×3 | 20 | 20 | 3 |
| | Lh-25×25×3 | 25 | 25 | 3 |
| | Lh-30×30×3 | 30 | 30 | 3 |
| | Lh-35×35×4 | 35 | 35 | 4 |
| Cold formed | Lc-20×20×2 | 20 | 20 | 2 |
| | Lc-25×25×2 | 25 | 25 | 2 |
| | Lc-30×30×2 | 30 | 30 | 2 |
| | Lc-35×35×3 | 35 | 35 | 3 |

Table 2 summarizes the value of above-mentioned material parameters. Mean value of Young's modulus was in the range of E = 205 GPa.

The set-up mounted on the testing machine, instrumentation and process control system (Fig. 3) allows the rig to operate in displacement as well as load control. The bending test samples, 480 mm long, were loaded with a pure bending moment in their central region, between inner rolls of four point (rolls) bending tool. The pure bending moment model appears to be particularly convenient for theoretical analysis of bending parameters. This kind of load was also chosen because it allowed the measurement of the cross-section distortion in a simple and precise way. During the bending tests orientation of beams arms were as in figure 1, in the aim to prevent buckling of arms, since in such orientation the free ends of beams arms undergo tensile stresses.

Two types of bending procedure were performed:

— continues bending up to visibly strain localization (first stage of beam collapse), to determine the bending moment as a function of curvature,

— step by step loading and unloading, to determine the springback coefficient as a function of bending radius.

TABLE 2

Mechanical material properties of angle-section beams made of St3S common steel

| | | $R_e$, MPa | n | C, MPa | $\varepsilon_0$ |
|---|---|---|---|---|---|
| Hot rolled | Lh-20×20×3 | 295 | 0,062 | 467 | -0,044 |
| | Lh-25×25×3 | 291 | 0,065 | 471 | -0,046 |
| | Lh-30×30×3 | 303 | 0,064 | 481 | -0,026 |
| | Lh-35×35×4 | 299 | 0,059 | 463 | -0,041 |
| Cold formed | Lc-20×20×2 | 351 | 0,096 | 588 | -0,096 |
| | Lc-25×25×2 | 355 | 0,094 | 581 | -0,093 |
| | Lc-30×30×2 | 348 | 0,092 | 592 | -0,098 |
| | Lc-35×35×3 | 351 | 0,099 | 585 | -0,0104 |

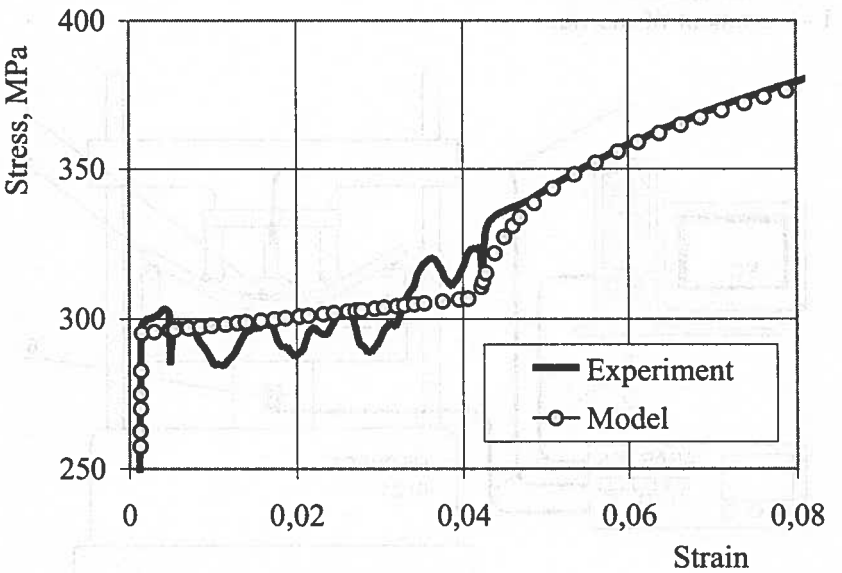


Fig. 2. Experimental and model tensile characteristic of St3S common steel

Based on the displacement and load measurements the bending radius (or curvature) and bending moment were calculated respectively. The bending radius was calculated as:

$$R = \frac{\left(\frac{a}{2}\right)^2 + h^2}{2h}, \tag{1}$$

where: a — width of sensor's base,
h — displacement sensor's core.

The bending moment acting on central region of specimen was calculated as:

$$M = \frac{Pb}{2}, \tag{2}$$

where: P — bending load,
b — distance between inner and outer bending rolls.

The bending curvature was calculated as inverse of bending radius— $\kappa = 1/R$. The value of springback coefficient K was calculated using the well known equation:

$$K = \frac{R}{R_s} = 1 - \frac{MR}{EI}, \tag{3}$$

where: $R)_s$ — specimen radius after unloading,
M — bending moment,
E — Young modulus,
I — moment of inertia.

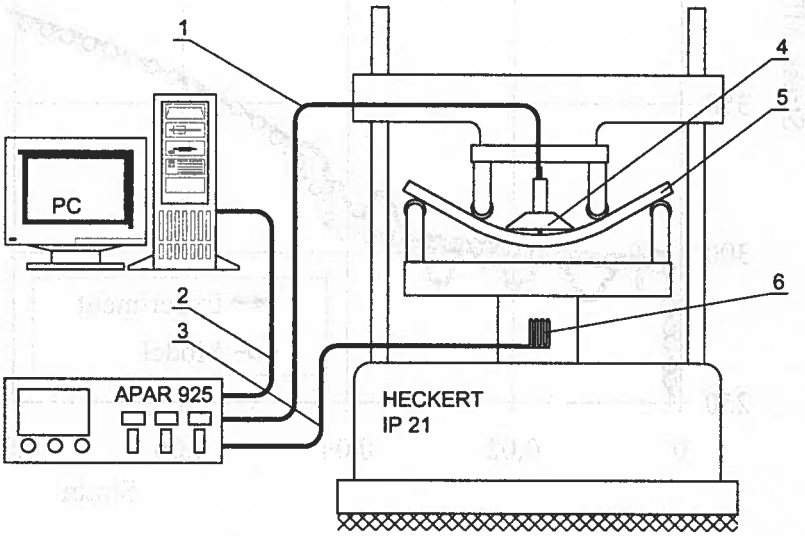


Fig. 3. Experimental set-up: 1 — displacement measuring path, 2 — RS 232 joint, 3 — load measuring path, 4 — inductive displacement sensor, 5 — specimen, 6 — load gauge

## 3. Experimental results and discussion

The bending characteristics, i.e. the relation between bending moment and curvature, demonstrate similar run, both in the case of the channel-section beams and angle-section beams (Fig. 4 and Fig. 5). At the first elastic stage of bending the bending

moment increase linearly with curvature increase. At the elastic-plastic range of bending the bending moment still increase with bending curvature due to strain hardening of a material, and reaches its maximum. At the next stage the bending moment started to decrease, as a result of cross- section distortion, and finally local beam collapse take place.

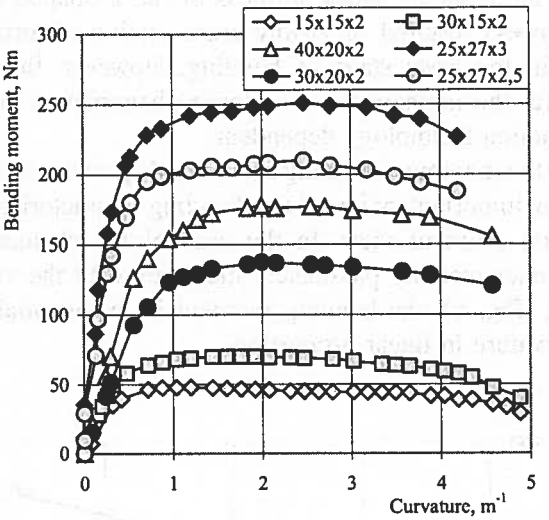


Fig. 4. Bending moment as a function of curvature for channel-section beams made of PA38 aluminium alloy

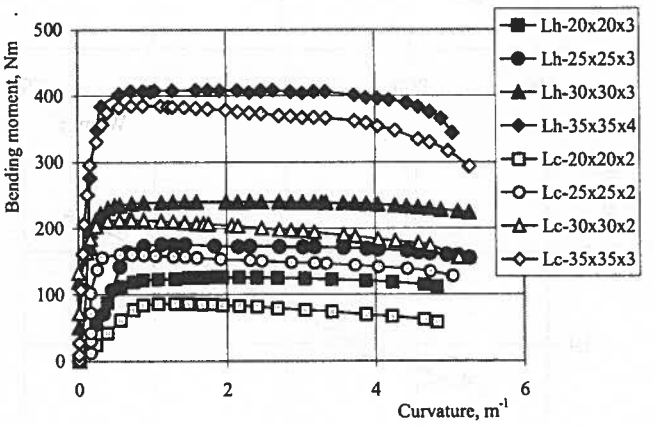


Fig. 5. Bending moment as a function of curvature for angle-section beams made of St3S common steel

In the case of channel-section beams the shape of bending characteristics depend on vertical wall height (Fig. 4). For shallow U-15×15×2 and U-30×15×2 beams the bending characteristic are flat in the wide range of curvature. For deep U- 25×27×2.5

and U-25×27×3 beams the intensity of bending moment change was the most visible, what was the result of the largest cross-section distortion.

When the angle-section beams are concerned the shape of bending characteristics depends first of all on the beam production method (Fig. 5). Cross-section stiffness of the L-shaped beams manufactured in hot rolling process is large and because of that, the bending process is more stable. Weak stiffness of the L-shaped beams manufactured in cold bending process resulted in visibly cross-section distortion (decrease of the bending moment) in the early stage of bending. However, the maximum value of bending curvature (at the moment when collapse phenomenon take place) seemed to be not on the production technology dependent.

The point, with the maximum bending moment $M_{max}$ and critical bending curvature ?cr coordinate is an important point of the bending characteristic from the bending technology designing point of view. In the case of the channel-section beams the value of these two characteristic parameters increases with the value of the sectional modulus increasing (Fig. 6), the bending moment in exponential proportion and the critical bending curvature in linear proportion.

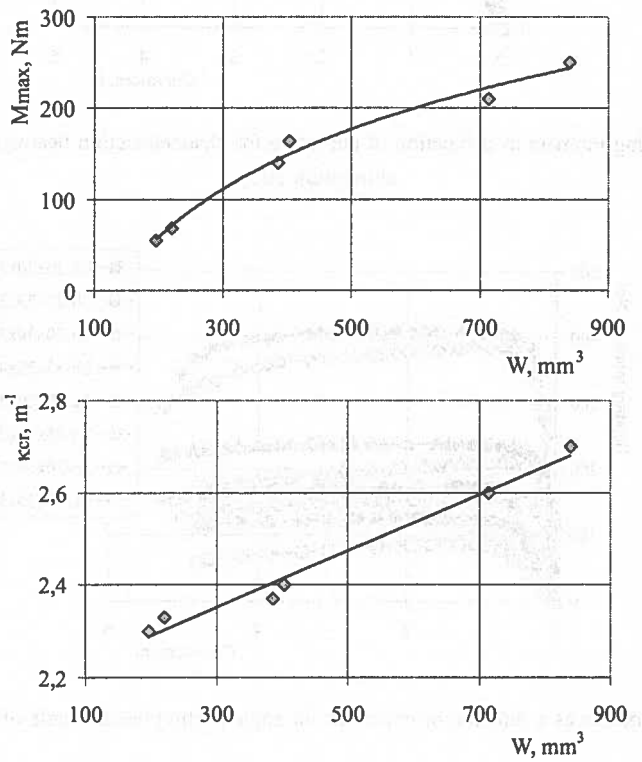


Fig. 6. Maximum bending moment (upper) and critical bending curvature (lower) dependence on the sectional modulus of U-shaped beams

When the angle-section beams are concerned similar relation was found only in the case of the maximum bending moment, which increases in linear proportion with the value of the sectional modulus increasing (Fig. 7). For cold-formed L-shaped beams increase in the value of the bending moment was more intensive than for hot-formed beams. Statistical elaboration of experimental results enabled to find linear relation between the value of critical bending curvature and the beams wall height to wall thickness (H/t) ratio. Taking into account this presentation (Fig. 8) the effect of beams production technology is evidently demonstrated. The value the critical bending curvature of cold-formed L-shaped beams seemed to be twice smaller than that of hot-formed beams.

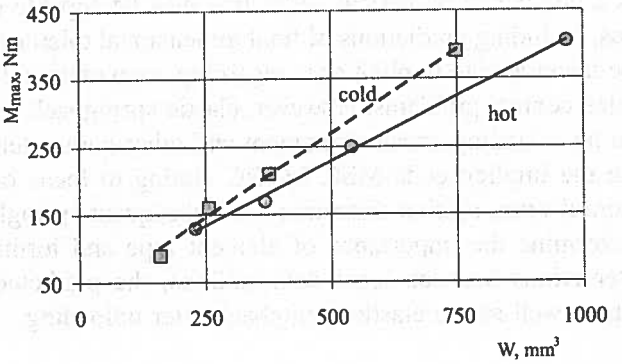


Fig. 7. Maximum bending moment dependence on the sectional modulus of L-shaped beams

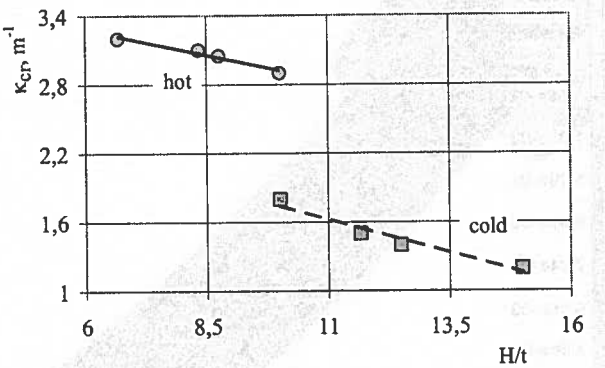


Fig. 8. Critical bending curvature dependence on the H/t ratio of L-shaped beams

## 4. Numerical procedure

Numerical simulation of bending is a rather delicate task. Plasticity effects in material, contact between specimen and tool, and springback during unloading involve

modelling challenges. Basically, FEM implementations can be considered as either implicit or explicit. Implicit algorithms solve the time-dependent non-linear problem directly by use of a predictor- corrector method, e.g. Newton-Raphson iteration scheme. The stiffness matrix is thus updated through the entire analysis, and the solution can under normal circumstances be regarded as correct within the error introduced by e.g. discretisation and the constitutive formulation. In explicit codes, no equilibrium check is performed during the analysis, i.e. the corrector step is omitted. Drift from the correct solution may thus be a problem. However, stability requirements reduce this problem as the time steps have to be satisfactory small. Generally, explicit codes are preferred in analyses of transient dynamics such as impact problems.

There exists a number of numerical codes that may be capable of handling forming type problems, including predictions of final dimensional tolerances. Explicit codes have proven to be favourable to implicit ones regarding computational efficiency, particularly for large size contact problems. However, elastic springback results are reported to be sensitive to mass scaling, mesh refinement and other parameters [9, 10]. For this reason, we chose the implicit code MSC MARC aiming to focus on parameters that affected prediction of cross-section distortion and subsequent springback. Efforts have been made to determine the importance of element type and formulation. Attention is placed on interactions between local deformations, the predicted stress state and bending moment, as well as the elastic springback after unloading.

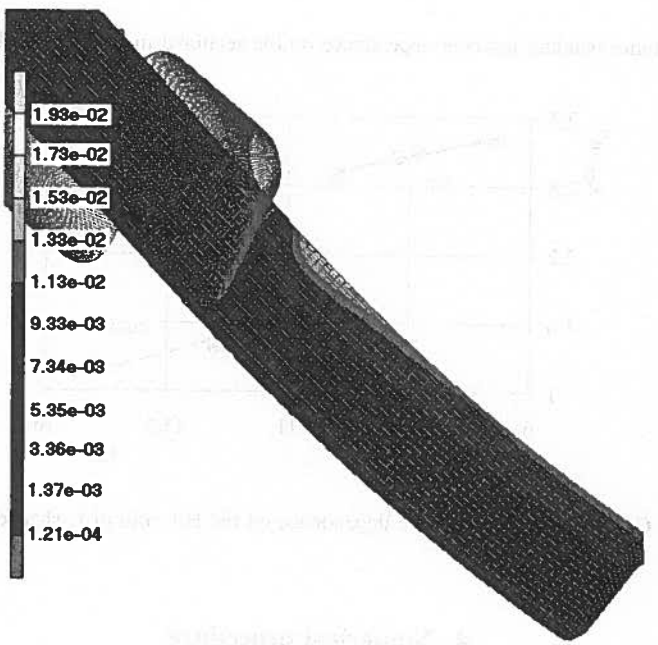


Fig. 9. Side view of the finite element model of the L-shaped beam and cross-sectional strain distribution at bending radius R = 0.76 m

Allowing only for symmetrical bending modes such that two-plane symmetry can be assumed, one quarter of the specimen was modelled by brick elements, in the case of both the channel-section beams (Fig. 9) and angle-section beams (Fig. 10). In the case of brick elements, the assumed strain formulation [11] and full integration elements were used separately to improve the bending behaviour of those elements. Bended specimens were in contact with rolls which were idealised as rigid with no friction force exist on contact surface. An automatic mesh program was applied in this work to generate the finite-element mesh grid.

Numerical calculation was performed in the case of the Lh-20×20×3 angle- section beam made of St3S common steel and the U-25×27×3 channel-section beam made of PA38 aluminium alloy. Similar to experimental investigations two types of modeling procedure of bending process was performed:

— continues bending up to visibly strain localization (first stage of beam collapse), to determine the bending moment as a function of curvature,
— step by step loading and unloading, to determine the springback coefficient as a function of bending radius.

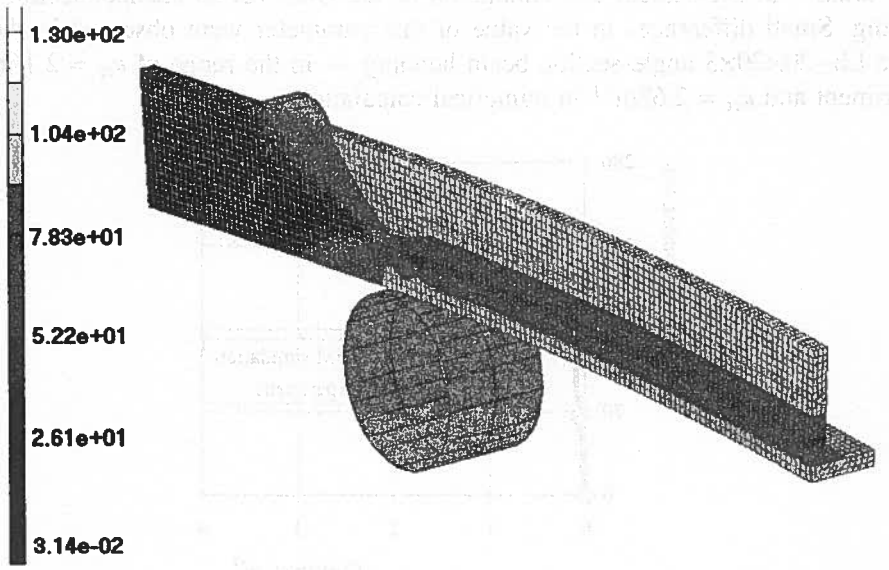


Fig. 10. Side view of the finite element model of the U-shaped beam and cross-sectional stress distribution at bending radius R = 0.90 m

Convergence of numerical solution was evaluated on the base of four different models with different amount and dimension of mesh elements. Rough model amounts 3,920 elements when the most precise model amounts 9,600 elements. From the economical point of view (calculation precision versus calculation time) the model which amounts 7,700 elements was satisfactory.

Numerical results have shown that stress distribution across cross-section of both, the L-shape and U-shape beams was uniform on whole specimen length between inner bending rolls, what confirms the assumption of pure bending moment loading. Only for small bending radius a local strain concentration near bending roll was observed (Fig. 9).

## 5. Comparison of experimental and calculated results

The bending characteristics obtained on the base of experimental results and numerical calculations have shown quite good correlation (Fig. 11 and Fig. 12), however the calculated bending characteristic overestimates experimental one. For the U-25×27×3 channel-section beam made of PA38 aluminium alloy the largest difference in the value of maximum bending moment amounts 7.2%, while for the Lh-20×20×3 angle- section beam made of St3S common steel this difference amounts 12.6%. Larger difference in the case of L-shaped beam its more complicated cross-section geometry, less precise described in FE model. The critical bending curvature amounts $\kappa_{cr} = 2.2\text{m}^{-1}$ in experiment and simulation of the U-25×27×3 channel-section beam bending. Small differences in the value of this parameter were observed in the case of the Lh- 20×20×3 angle-section beam bending — in the range of $\kappa_{cr} = 2.16\text{m}^{-1}$ in experiment and $\kappa_{cr} = 2.68\text{m}^{-1}$ in numerical calculations.

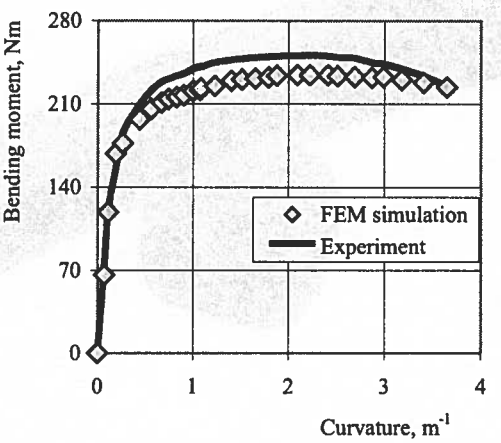


Fig. 11. Bending characteristic of the U-25×27×3 channel-section beam made of PA38 aluminium alloy — comparison between experimental and numerical results

Since there is a close relation between the bending moment and the springback coefficient, described by equation (3), it should be expected that calculated values of springback coefficient amount larger value than experimental one. Comparison of calculated and experimental springback characteristics (Fig. 13 and Fig. 14) confirm this observation. Difference between experimental and calculated K-value decrease

with bending curvature increasing (i.e. the bending moment decreasing) as a result of the elastic zone on beam cross- section decreasing. The larger values of springback coefficients for the L-shaped beam (Fig. 14) in comparison with the U-shaped beam (Fig. 13) resulted from difference in the Young's modulus value — E = 205 GPa for the St3S common steel and E = 80.7 for the PA38 aluminium alloy.

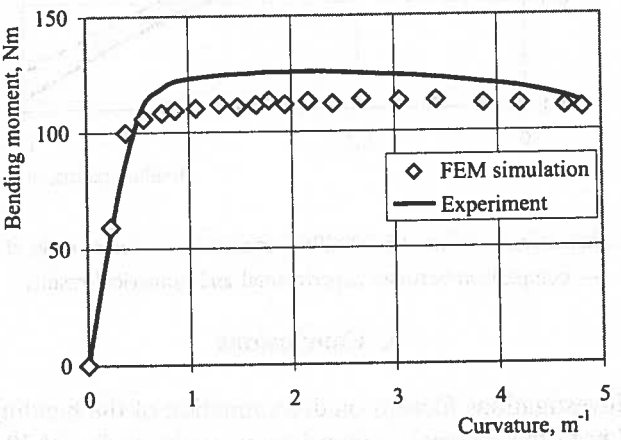


Fig. 12. Bending characterictic of the Lh-20×20×3 angle-section beam made of St3S common steel — comparison between experimental and numerical results

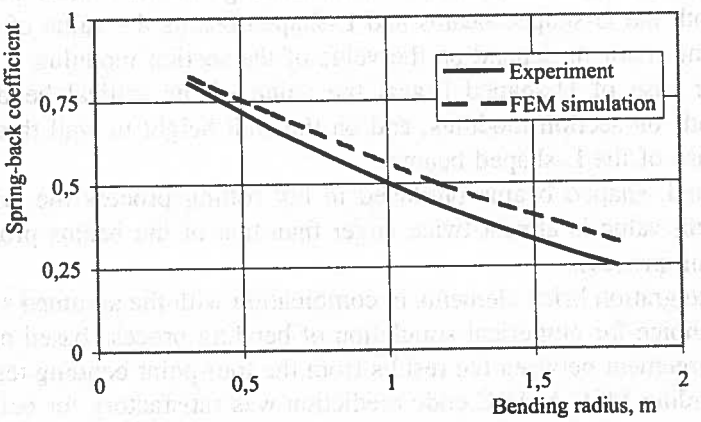


Fig. 13. Sprinback characterictic of the U-25×27×3 channel-section beam made of PA38 aluminium alloy — comparison between experimental and numerical results

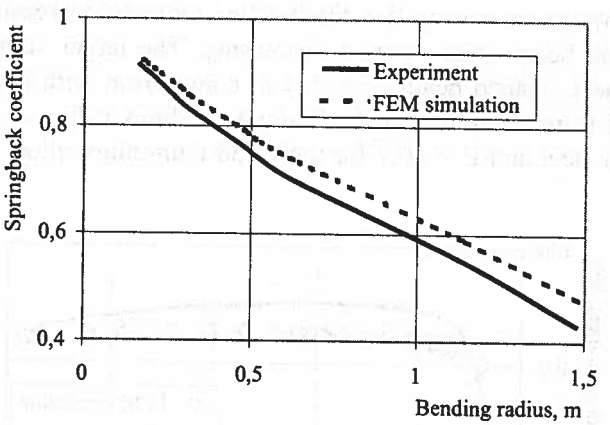


Fig. 14. Springback characteristic of the Lh-20×20×3 angle-section beam made of St3S common steel — comparison between experimental and numerical results

## 6. Conclusions

The present investigations focuses on determination of the bending and springback characteristics of both the channel-section beams made of the PA38 aluminium alloy and angle-section beams made of the St3S common steel. Based upon the experimental results and the numerical simulation of bending process the following conclusions can be drawn:

- proceeding of the bending characteristics, i.e. bending moment versus bending curvature relation, depend on both the strain hardening of profile material and cross-section distortion increase with bending curvature increasing,
- for both the U-shaped beams and L-shaped beams the value of the maximum bending moment depend on the value of the section modulus,
- in the case of U-shaped beams the value of the critical bending curvature depends on section modulus, and on the wall height to wall thickness ratio in the case of the L-shaped beams,
- for the L-shaped beams produced in hot rolling process the critical bending moment value is almost twice larger than that of the beams produced in cold forming process,
- full integration brick elements in combination with the assumed strain is preferable choice for numerical simulation of bending process based on FEM,
- the agreement between the results from the four-point bending test and the corresponding MSC MARC code prediction was satisfactory for both the bending and springback characteristics.

**Acknowledgements**

Gratitude is expressed to the State Committee for Scientific Research for financial support under contract No. PRz-U-5915/DS.

REFERENCES

[1] W.D. Franz, Das Kaltbiegen von Rohren, Springer Verlag, Berlin-Göttingen- Heilderberg 1961.

[2] Y. Xu, L.C. Zhang, T.X. Lu, The elastic-plastic pure bending and springback of L-shaped beams, Int. J. Mech. Sci. **29**, 425 (1987).

[3] T.X. Yu, L.S. The, Large plastic deformation of beams of angle-section under symmetric bending, Int. J. Mech. Sci. **39**, 829 (1997).

[4] A.A. El-Domiaty, A.A. Elsharkawy, Stretch-bending analysis of U-section beams, Int. J. Mach. Tool Manufac. **38**, 75 (1997).

[5] A.A. El-Domiaty, A.A. Elsharkawy, Determination of stretch-bendability limits and springback for T-section beams, J. Mat. Proc. Technol. **110**, 265 (2001).

[6] T. Welo, F. Paulsen, Local flane buckling and its relation to elastic springback in forming of aluminium extrusions, J. Mat. Proc. Technol. **60**, 149 (1996).

[7] F. Micari, A. Forcelesse, L. Fratini, F. Gabrielli, N. Alberti, Springback evaluation in fully 3-D sheet metal forming processes, Annals of CIRP **46**, 167 (1997).

[8] A.H. Clausen, O.S. Hopperstad, M. Langseth, Stretch bending of aluminium extrusions, Int. J. Appl. Mech. Engn. **7**, 7 (2002).

[9] K. Mattiasson, A. Strang, P. Thiderkvist, A. Samuelsson, Simulation of springback in sheet metal forming, Proc. NUMIFORM, 115 (1995).

[10] S.W. Lee, D.Y. Yang, An assessment of numerical parameters influencing springback in explicit finite element analysis of sheet metal forming process, J. Mat. Proc. Technol. **80-81**, 60 (1998).

[11] MSC Software, MSC Marc Element Library, Santa Ana 2000.

*Received: 10 April 2004.*